CRREL
REPORT 85-12

US Army Corps of Engineers
Cold Regions Research & Engineering Laboratory

Analysis of river wave types

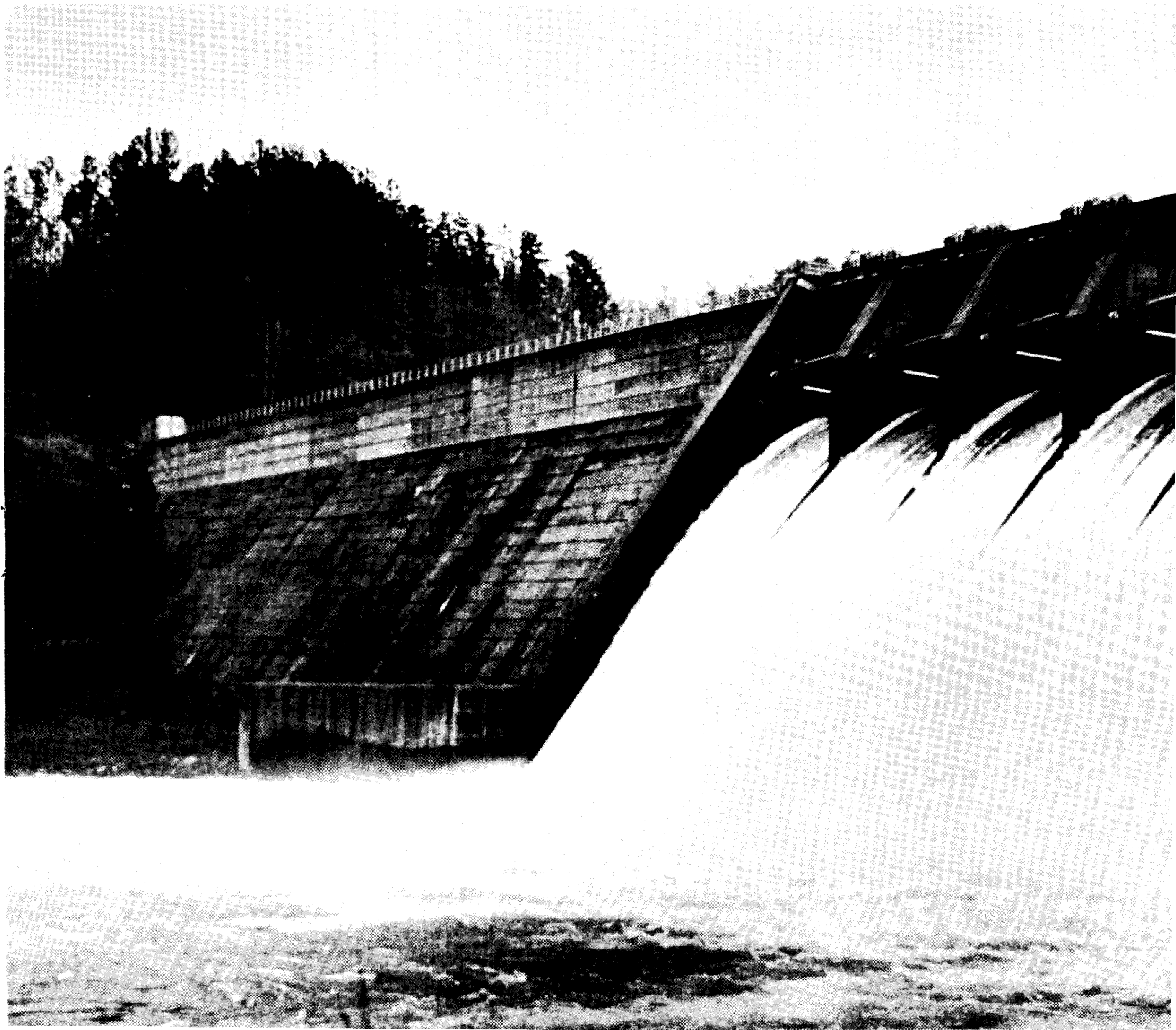

CRREL Report 85-12

June 1985

Analysis of river wave types

Michael G. Ferrick

Prepared for
OFFICE OF THE CHIEF OF ENGINEERS

REPORT DOCUMENTATION PAGE

READ INSTRUCTIONS BEFORE COMPLETING FORM

1. REPORT NUMBER: CRREL Report 85-12	2. GOVT ACCESSION NO.
3. RECIPIENT'S CATALOG NUMBER	
4. TITLE (and Subtitle): ANALYSIS OF RIVER WAVE TYPES	5. TYPE OF REPORT & PERIOD COVERED
	6. PERFORMING ORG. REPORT NUMBER
7. AUTHOR(s): Michael G. Ferrick	8. CONTRACT OR GRANT NUMBER(s): DA Project 4A762730AT42, Work Unit 003
9. PERFORMING ORGANIZATION NAME AND ADDRESS: U.S. Army Cold Regions Research and Engineering Laboratory, Hanover, New Hampshire 03755-1290	10. PROGRAM ELEMENT, PROJECT, TASK AREA & WORK UNIT NUMBERS
11. CONTROLLING OFFICE NAME AND ADDRESS: Office of the Chief of Engineers, Washington, D.C. 02314	12. REPORT DATE: June 1985
	13. NUMBER OF PAGES: 24
14. MONITORING AGENCY NAME & ADDRESS (if different from Controlling Office)	15. SECURITY CLASS. (of this report): Unclassified
	15a. DECLASSIFICATION/DOWNGRADING SCHEDULE

16. DISTRIBUTION STATEMENT (of this Report)

Approved for public release; distribution is unlimited.

17. DISTRIBUTION STATEMENT (of the abstract entered in Block 20, if different from Report)

18. SUPPLEMENTARY NOTES

19. KEY WORDS (Continue on reverse side if necessary and identify by block number)

Dam breach	Rivers	Waves
Dimensionless scaling parameters	Rosenblueth method	
Hydropower peaking	Saint-Venant equations	
River ice	Unsteady flow	

20. ABSTRACT (Continue on reverse side if necessary and identify by block number)

In this paper, we consider long-period, shallow-water river waves that are a consequence of unsteady flow. River waves result from hydroelectric power generation or flow control at a dam, the breach of a dam, the formation or release of an ice jam, and rainfall/runoff processes. The Saint-Venant equations are generally used to describe river waves. Dynamic, gravity, diffusion, and kinematic river waves have been defined, each corresponding to different forms of the momentum equation and each applying to some subset of the overall range of river hydraulic properties and time scales of wave motion. However, the parameter ranges corresponding to each wave description are not well defined, and the transitions between wave types have not been explored. This paper is an investigation into these areas, which are fundamental to

20. Abstract (cont'd).

river wave modeling. The analysis is based on the concept that river wave behavior is determined by the balance between friction and inertia. The Saint-Venant equations are combined to form a system equation that is written in dimensionless form. The dominant terms of the system equation change with the relative magnitudes of a group of dimensionless scaling parameters that quantify the friction/inertia balance. These scaling parameters are continuous, indicating that the various types of river waves and the transitions between them form a spectrum. Additional data describing the physical variability of rivers and waves are incorporated into the analysis by interpreting the scaling parameters as random variables. This probabilistic interpretation provides an improved estimate of the friction/inertia balance, further insight into the continuous nature of wave transitions, and a measure of the reliability of wave type assessments near a transition. Case studies are used to define the scaling parameter ranges that represent each wave type and transition, and to provide data with which to evaluate the usefulness of the analysis for general application.

PREFACE

This report was prepared by Michael G. Ferrick, Hydrologist, of the Snow and Ice Branch, Research Division, U.S. Army Cold Regions Research and Engineering Laboratory. Funding for this research was provided by DA Project 4A762730AT42, *Design, Construction and Operations Technology for Cold Regions,* Work Unit 003, *Winter Battlefield River Mechanics.*

The author thanks Hung Tao Shen and Hayley H. Shen for technically reviewing this report and Maria Bergstad for careful editing. Earl Edris of the U.S. Army Waterways Experiment Station programmed the Rosenblueth and β-distribution routines that were used in the report.

CONTENTS

ILLUSTRATIONS

Figure

TABLES

Table

NOMENCLATURE

a	minimum value of random variable
A_0	initial wave amplitude
b	maximum value of random variable
B	beta function
c	shallow-water wave celerity
c_d	celerity of diffusion waves
c_k	celerity of kinematic waves
c_m	measured wave celerity
C_r	Courant number, scaling parameter of the Saint-Venant system equation
C_*	dimensionless Chezy conveyance coefficient
D	dimensionless diffusion coefficient
D_I	scaling parameter of the Saint-Venant system equation
$E[y]$	expected value of random variable y
$f(y)$	β distribution of random variable y
F_c, F_I	friction scaling parameters of the Saint-Venant system equation
F_0	Froude number
g	acceleration due to gravity
i	$\sqrt{-1}$
k	variable relating depth to hydraulic radius; arbitrary constant
k_1, k_2	constants
$P[y < x]$	probability that random variable y is less than x
R	hydraulic radius of the channel
R_1, R_2	reliability estimates
S	slope ratio
S_f	energy gradient or friction slope of the flow
S_0	river bed slope
S_x	standard deviation of random variable x
t	time
t^*	dimensionless time
v	flow velocity
v_0	velocity scaling variable
v^*	dimensionless velocity
V_x	coefficient of variation of random variable x
x	longitudinal distance
x^*	dimensionless distance
y	flow depth
y_0	depth scaling variable
y^*	dimensionless depth
α, β	parameters of a β distribution
Δt	time scaling variable
Δx	length scaling variable
γ	coefficient of exponential amplitude decay of reservoir waves
ρ	correlation coefficient

ANALYSIS OF RIVER WAVE TYPES

Michael G. Ferrick

INTRODUCTION

Long-period waves in rivers are a consequence of unsteady flow, which may occur as a result of hydroelectric power generation or flow control at a dam, the breach of a dam, the formation or release of an ice jam, or rainfall/runoff processes. River waves have flow depths that are several orders of magnitude smaller than their wavelengths, so they are classified as shallow-water waves. The study of river waves is complicated by the hydraulic properties of rivers and the time scales of the wave motion, which range over several orders of magnitude. Natural rivers vary greatly in size and in discharge. Impounded rivers are both wider and deeper than they were in their natural state, and they have diverse hydraulic properties. Flood waves in large river systems develop over several days, while those in some small rivers can form in several minutes. Flow control and hydroelectric turbine gates may be adjusted rapidly, creating abrupt flow waves both upstream in the reservoir and downstream in the tailwater river. Because of this diversity, general physical insights regarding river waves are elusive.

Observations indicate that river waves are a primary cause of river ice cover breakup. Therefore, a theory describing the interactions between a river wave and the ice cover would have great practical importance. When a river becomes covered with ice, frictional energy dissipation increases, but the effect of this increased friction on river wave behavior has not been established. This understanding is a prerequisite to the development of theories of ice cover stability in the presence of river waves.

The Saint-Venant equations of continuity and momentum are generally used to describe unsteady flow in rivers. Within this basic model, river waves may be classified as dynamic, gravity, diffusion, or kinematic waves, corresponding to different forms of the momentum equation. Dynamic waves are described by retaining all terms of the momentum equation. As is typical of shallow-water waves, dynamic river waves have a celerity that is related to the water depth. The momentum equation for gravity waves ignores the effects of bed slope and viscous energy losses; gravity waves propagate at the dynamic wave celerity and their flows are dominated by inertia. Diffusion and kinematic waves are at the opposite extreme. The diffusion wave momentum equation ignores inertia, and the kinematic wave equation ignores both inertia and the pressure gradient caused by varying flow depths over distance. Both of these wave types travel at a celerity governed by the frictional resistance of the river bed. This celerity is related to the velocity of the flow and is significantly slower than the dynamic wave celerity. Diffusion and kinematic wave propagation requires the movement of a large quantity of water. In this paper these waves are frequently grouped together and are called bulk waves.

Our present understanding of the relationships between various river wave types is based on linear stability theory (Ponce and Simons 1977, Menéndez and Norscini 1982). This linear theory provides useful, but largely qualitative, insights into the behavior of each wave type, and the transitions between wave types are not considered: waves of a given type include or exclude specific terms or processes in the momentum balance. The concept of step changes between river wave types is not reasonable. There

must be cases that are intermediate between wave types, suggesting the need for a treatment of wave transitions. Wave types are identified either by using the linear theory or by comparing magnitudes of normalized terms of the dynamic wave momentum equation (Henderson 1963, Woolhiser and Liggett 1967), and then applying judgment to interpret the results.

The object of this paper is a) to develop a quantitative method for identifying river wave types and b) to clarify the relationships between wave types. The analysis is based on the principle that the balance between friction and inertia determines river wave behavior. The Saint-Venant equations are combined to form a system equation. Written in dimensionless form, the system equation provides scaling parameters that quantify the magnitudes of all terms in the equation and indicate the relative importance of friction, inertia, and pressure gradient effects on a wave. By interpreting the scaling parameters probabilistically, additional data can be incorporated into the analysis to account for the variable physical characteristics of a river and a wave. This more general interpretation provides an improved estimate of the friction/inertia balance, insight into the continuous nature of transitions between wave types, and a measure of the reliability of wave type assessments near a transition. Finally, we identify the scaling parameter ranges that correspond to each wave type and transition with data from case studies. These case studies encompass a wide range of river and wave conditions, attesting to the general utility of the approach.

BACKGROUND

Courant and Friedrichs (1948) noted the analogy between nonlinear wave motion in gases and in shallow water, and they developed the mathematics to treat first-order, quasi-linear hyperbolic flow equations for functions of two independent variables. Continuity of all functions and all required derivatives of these functions was assumed. Stoker (1957) applied this theory to the study of river flow waves, providing the mathematical and conceptual basis for our present understanding of river waves. Following Stoker, we consider an idealized river with a wide rectangular prismatic channel and no local inflow. The Saint-Venant equations of mass conservation and momentum balance are then written

$$\frac{\partial y}{\partial t} + v\,\frac{\partial y}{\partial x} + y\,\frac{\partial v}{\partial x} = 0 \qquad (1)$$

$$\frac{\partial v}{\partial t} + v\,\frac{\partial v}{\partial x} + g\left(\frac{\partial y}{\partial x} - S_0 + S_f\right) = 0 \qquad (2)$$

where y = the flow depth (m)
v = the flow velocity (m/s)
g = acceleration due to gravity (m/s^2)
S_0 = the river bed slope
S_f = the energy gradient of the flow
x = the longitudinal distance (m)
t = time (s).

Stoker transformed eq 1 and 2 into their characteristic form:

$$v + 2c + g(S_f - S_0)\,t = k_1 \qquad (3)$$

$$\text{along} \quad \frac{dx}{dt} = v + c,$$

and

$$v - 2c + g(S_f - S_0)\,t = k_2 \qquad (4)$$

$$\text{along} \quad \frac{dx}{dt} = v - c,$$

where $c = \sqrt{gy}$ defines the shallow-water surface wave celerity and k_1 and k_2 are constants. The solutions of $dx/dt = v \pm c$ yield two distinct sets of curves in the x–t plane, called characteristics. The inverse slopes of these curves define the dynamic wave celerity, that is, the speed of shallow-water waves in a flowing stream. The dynamic wave celerity is independent of the river bed and energy slopes, and appears to be the only wave speed contained in the governing equations.

The momentum equation describing a gravity wave is obtained from eq 2 by omitting the river bed slope and energy gradient terms. The theory of characteristics can also be applied for these waves, and the resulting equations are simplified forms of eq 3 and 4:

$$v + 2c = k_1 \quad \text{along} \quad \frac{dx}{dt} = v + c, \qquad (5)$$

$$v - 2c = k_2 \quad \text{along} \quad \frac{dx}{dt} = v - c, \qquad (6)$$

Waves described by eq 5 and 6 have been termed "simple" waves. Gravity waves are undamped and propagate at the dynamic wave celerity.

The diffusion wave momentum equation is obtained by neglecting the inertia terms [$\partial v/\partial t$, $v(\partial v/\partial x)$] in eq 2. Differentiating both this momentum equation and eq 1 with respect to x, and differentiating the momentum equation with respect to t, yields three equations that are combined with eq 1 to eliminate derivatives of the depth. The Chezy equation, with dimensionless conveyance coefficient C_* assumed constant, is used to describe the energy slope. Performing these operations yields

$$\frac{\partial v}{\partial t} + c_d \frac{\partial v}{\partial x} = D \frac{\partial^2 v}{\partial x^2} \tag{7}$$

where

$$c_d = \frac{5}{2} v - \frac{gC_*^2 RS_0}{v} \text{ and } D = \frac{gC_*^2 Ry}{2v}.$$

Equation 7 is an advective-diffusion equation with R the hydraulic radius of the channel. If we retain the wide-channel assumption, the hydraulic radius is equivalent to y/k, where $k = 1$ for open water conditions and $k = 2$ if the channel is covered with ice.

The kinematic wave momentum equation is obtained by omitting the inertia and the derivative of depth with distance ($\partial y/\partial x$) terms in eq 2. Then, proceeding as with diffusion waves yields the well-known kinematic wave equation

$$\frac{\partial v}{\partial t} + c_k \frac{\partial v}{\partial x} = 0, \tag{8}$$

where

$$c_k = \frac{3}{2} v.$$

The important distinction between the bulk waves is that diffusion waves attenuate, while kinematic waves do not.

Comparing eq 3 through 8, we find that the equation for river wave celerity changes with the form of the momentum equation that is used. The celerities of diffusion and kinematic waves are both related to the velocity of the flow. The celerities of these bulk waves are typically much smaller than the dynamic wave celerity and are generally lumped together and termed the kinematic wave celerity.

Stoker (1957) argued that because the equations describing dynamic waves are more general, imperceptible dynamic waves, or "forerunners," must occur simultaneously when the primary wave is kinematic. This concept of an ever-present role for dynamic waves in river flow mechanics is widely accepted. Therefore, river wave studies based upon "simplified" gravity, diffusion, and kinematic wave equations are perceived as inherently less accurate than those using the more complete dynamic wave equations.

The governing equations for each wave type are nonlinear, and the geometry of natural channels is highly variable. These conditions generally require that numerical solutions be used to describe river waves. The algorithms typically chosen to solve the dynamic wave equations in applications use first- or second-order accurate difference approximations and coarse numerical meshes. The solutions obtained with these models therefore include significant errors, due to truncation and discretization, that cause numerical diffusion and dispersion of the solution. When the effects of certain physical processes are small relative to other processes, the terms of the governing equation have widely different magnitudes. Equations of this type are termed "stiff," and are difficult to solve numerically. Woolhiser and Liggett (1967) reported numerical difficulties that resulted from modeling predominantly kinematic waves using dynamic wave characteristic equations. The stability of explicit numerical methods depends on the dynamic wave celerity, even for cases where the inertia terms are negligible. When stability problems occur, the cure is often achieved by increasing numerical diffusion in the algorithm, further degrading the accuracy of the solution. Taken together, these considerations imply that more complete equations may not yield more accurate river wave simulations.

The problems associated with universal application of the dynamic wave equations suggest the alternative approach of using physical insight to identify an appropriate wave type. However, wave types cannot at present be identified with a known degree of certainty. For example, Cunge et al. (1980) stated that rapidly varying river flows require the use of the dynamic wave equations, but Ferrick et al. (1984) studied a large number of instantaneous flow releases in two rivers and found that in all cases the inertia of the flow was negligible. The logic linking rapid flow variation with inertia is clear but insufficient to ensure dynamic wave behavior. The converse example is that slowly developing, long-period floods behave as kinematic waves. A more quantitative representation of the roles of friction and inertia would make it possible to characterize and identify river wave types.

ANALYSIS

River waves propagating at the dynamic and kinematic wave celerities are generally observed in different situations. In impounded rivers, where depth is much greater than wave amplitude, observed wave celerities are those of dynamic waves (Ferrick and Waldrop 1977, Ferrick 1979), but wave propagation observed in free-flowing rivers is more commonly at the kinematic wave celerity (Ferrick et al. 1984). These observations suggest that it may be possible to distinguish between bulk and dynamic waves simply by measuring and classifying wave celerity.

We might also reason that river waves are shallow-water waves of extremely long wavelength. A depth parameter nondimensionalized by wavelength, which follows from the simple harmonic small-amplitude wave theory of ocean gravity waves, differentiates between deep-water and shallow-water conditions. Extending these ocean wave classification ideas to rivers, in light of typical wavelength differences between rapidly and gradually varying flows, suggests that a dimensionless depth or a dimensionless wavelength may be indicative of wave type.

A connection between the form of the momentum equation and the physical characteristics of a river and wave would provide a means to identify wave type and would clarify the relationships between waves. Each of the river-wave types that have been identified is described by equations that are subsets of the Saint-Venant equations. To consider the behavior of solutions of this equation system, we will assume that the functions describing depth and velocity possess continuous second derivatives and that the river bed slope is constant. Then, differentiating eq 1 and 2 with respect to distance x, differentiating eq 2 with respect to time t, and combining these three equations with eq 1 and 2 to eliminate the depth derivative terms yields a system equation:

$$\frac{\partial^2 v}{\partial t^2} + 2v\frac{\partial^2 v}{\partial x \partial t} + (v^2 - gy)\frac{\partial^2 v}{\partial x^2} + \left(\frac{2v}{C_*^2 R}\right)\frac{\partial v}{\partial t} + \left[\frac{5v^2}{C_*^2 R} - 2gS_0 + 3\left(\frac{\partial v}{\partial t} + v\frac{\partial v}{\partial x}\right)\right]\frac{\partial v}{\partial x} = 0 \qquad (9)$$

in which the Chezy equation with constant C_* is again used to describe the energy slope. The second-order terms in eq 9 follow from the inertia and pressure gradient terms in eq 2. The quasi-linear first-order terms result from the energy or friction slope and the bed slope terms, and the nonlinear first-order terms are due to inertia. This system equation has the form

$$A(x, t)\frac{\partial^2 v}{\partial t^2} + 2B(x, t)\frac{\partial^2 v}{\partial x \partial t} + C(x, t)\frac{\partial^2 v}{\partial x^2} = f\left(v, \frac{\partial v}{\partial x}, \frac{\partial v}{\partial t}, x, t\right). \qquad (10)$$

The second-order terms in second-order differential equations are generally of principal significance. As $B^2 - AC$ is greater than zero, eq 9 is hyperbolic with a pair of characteristic curves (Hildebrand 1962) defined by

$$A\left(\frac{dx}{dt}\right)^2 - 2B\left(\frac{dx}{dt}\right) + C = 0. \qquad (11)$$

Solving eq 11 for dx/dt again yields the dynamic wave celerity $v \pm c$ as the inverse slope of the characteristics.

The assumption implicit in the development of eq 3 and 4 is that all the processes represented in eq 2 are of comparable magnitude. However, from the perspective of the system equation, the behavior of a river wave must depend on the relative contributions of inertia, friction, and pressure. When inertia is significant, dynamic waves are of primary importance in river flow mechanics, as indicated by eq 3 and 4. The role of dynamic waves diminishes with the relative importance of inertia. Bulk wave behavior indicates that the second-order terms of eq 9 are dominated by the quasi-linear first-order terms; that is, friction dominates inertia.

An evaluation of the relative magnitudes of the terms in eq 9 and a basis for interpreting these results would provide a quantitative measure of the importance of each process in the momentum balance and would indicate the wave type. Writing eq 9 in dimensionless form permits an assessment of these relative magnitudes. Introducing parameters $v_0, y_0, \Delta x$, and Δt, which are in some sense characteristic of the flow and wave motion, we rewrite eq 9 in terms of dimensionless variables $v^* = v/v_0$, $y^* = y/y_0$, $x^* = x/\Delta x$, and $t^* = t/\Delta t$ as

$$\frac{\partial^2 v^*}{\partial t^{*2}} + 2C_r v^*\frac{\partial^2 v^*}{\partial x^* \partial t^*} + (C_r^2 v^{*2} - D_I y^*)\frac{\partial^2 v^*}{\partial x^{*2}} + F_I\frac{v^*}{y^*}\frac{\partial v^*}{\partial t^*} + F_c\left(\frac{5}{2}\frac{v^{*2}}{y^*} - S\right)\frac{\partial v^*}{\partial x^*} + 3C_r\left(\frac{\partial v^*}{\partial t^*} + C_r v^*\frac{\partial v^*}{\partial x^*}\right)\frac{\partial v^*}{\partial x^*} = 0 \qquad (12)$$

where

$$C_r = \frac{v_0 \Delta t}{\Delta x} = \frac{v_0}{c_m}$$

$$D_I = \left(\frac{C_r}{F_0}\right)^2 = \frac{g y_0}{c_m^2} = \left(\frac{c}{c_m}\right)^2$$

$$F_I = \frac{2 C_r}{C_*^2} \left(\frac{k \Delta x}{y_0}\right)$$

$$S = \frac{S_0}{S_{f_0}}$$

$$F_0^2 = \frac{v_0^2}{g y_0} = \left(\frac{v_0}{c}\right)^2$$

$$F_c = F_I C_r$$

To proceed, we must define the physical scaling variables $v_0, y_0, \Delta x$, and Δt and evaluate S_0 and C_*. Mean velocity and depth characterize the flow and provide velocity and depth scales v_0 and y_0. The length scale that is important in the development of river waves is related to the wavelength. With mean flow depth as the depth scale, the comparable length scaling parameter Δx is the half-wavelength, and $k\Delta x/y_0$ appearing in parameters F_I and F_c is a dimensionless wavelength. The effect of friction on a wave is cumulative over the propagation distance. At distances less than a wavelength from the point of wave origin, Δx is taken as half the wave propagation distance. Δt is the time required for the wave to travel distance Δx. Therefore, $\Delta x/\Delta t$ is the measured wave celerity c_m. These three variables are evaluated with information from a pair of gauging stations. To obtain measured wave celerity, the river distance between the gauges is divided by the elapsed time between the wave arrivals. Wavelength is then obtained by multiplying wave celerity by the mean time for wave passage at the gauges. As the Chezy conveyance coefficient is depth-dependent, the most representative value of C_* for a reach is obtained from steady-flow stage measurements near the mean of the expected range. Finally, S_0 is evaluated as the mean bed slope of the river reach.

The fundamental dimensionless parameters of eq 12 are the Courant number C_r, the Froude number F_0, a friction parameter F_I, and the slope ratio S. Froude number F_0 represents a ratio of speeds, comparing the characteristic flow velocity to the surface wave celerity evaluated at the characteristic flow depth. With few exceptions, the range of Froude numbers for rivers is between 0 and 2, most commonly between 0 and 1. Slope ratio S compares the river bed slope to the energy gradient of the flow evaluated at the characteristic depth, velocity, and channel conveyance. For free-flowing rivers the value of the slope ratio is approximately 1. It is higher for reservoirs, where the presence of backwater significantly reduces the energy gradient.

The magnitudes of the terms in eq 12 directly reflect the importance of the physical processes they represent. The behavior of solutions of eq 12 can be assessed by considering C_r and F_I together with F_c and D_I, forming a group of dimensionless scaling parameters. Courant number C_r is composed of a characteristic flow velocity and length and time scales that are characteristic of the wave motion; it is the ratio of characteristic flow velocity to measured wave celerity, limiting the range of possible values to between 0 and 1. All terms in eq 12 except $\partial^2 v^*/\partial t^{*2}$ are functions of the Courant number. The terms having the Courant number as their dimensionless scaling parameter follow from the inertia terms of eq 2. The scaling parameter representing the largest inertia term cannot be larger than 3 and typically is about 1.

The effects of friction and bed slope on river flow are represented by the first-order terms with coefficients F_I and F_c. The values of these scaling parameters relative to 1 characterize the importance of friction in the momentum balance and, therefore, define the boundaries and govern the transitions between bulk, dynamic, and gravity wave types. F_c is related to the kinematic flow number obtained by Woolhiser and Liggett (1967) from a direct normalization of eq 2. Both measured wave celerity and dimensionless wavelength are components of F_I and F_c, though neither alone is adequate to characterize friction. The magnitudes of the friction parameters vary linearly with dimensionless wavelength. The measured wave celerity is a component of the Courant number. Bulk flow cases, where the flow velocity approaches the wave celerity, correspond to a large Courant number and increased relative magnitudes of the friction parameters. For the opposite condition of small flow velocity relative to measured wave celerity, the friction parameter magnitudes decrease due to their dependence on the Courant number, indicating a reduced role of friction relative to other processes. The other basic component of F_I and F_c is the dimensionless channel conveyance, which accounts for differences in the rate of energy dissipation between different river and flow situations.

F_c is presented in Figure 1 as a function of the

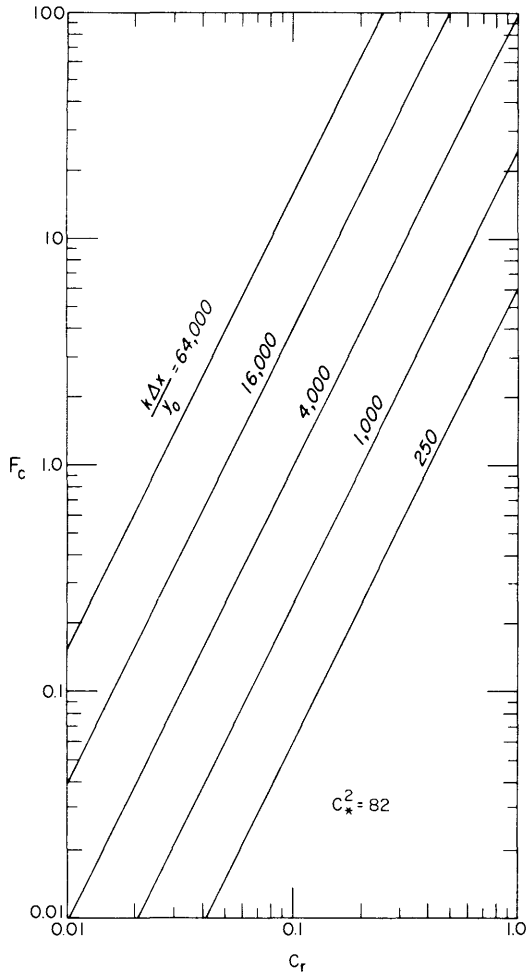

Figure 1. Friction scaling parameter F_c *as a function of Courant number for a range of dimensionless wavelengths and a typical dimensionless channel conveyance.*

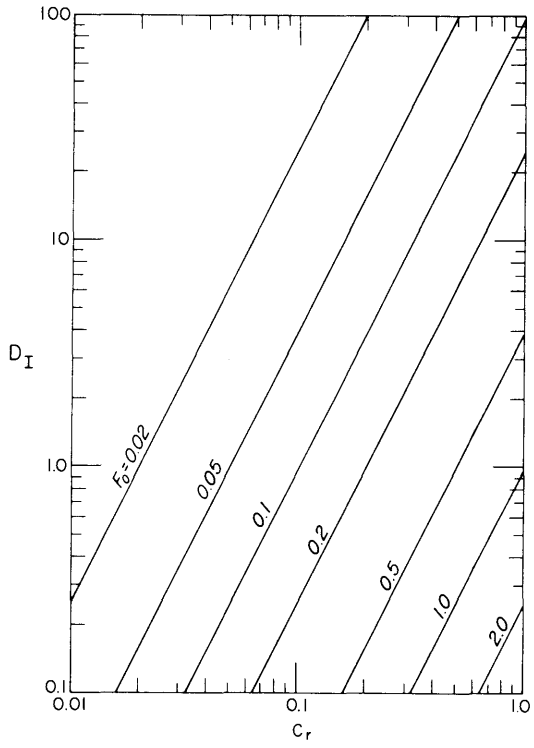

Figure 2. Scaling parameter D_I *as a function of Courant number for a range of Froude numbers.*

Courant number for a range of dimensionless wavelengths and an assumed dimensionless channel conveyance of about 9. Larger values of channel conveyance displace the band of curves to the right, corresponding to smaller F_c, with the converse true for smaller conveyances. Courant numbers greater than 0.4 and dimensionless wavelengths greater than 4000 are typical in natural rivers. For these conditions F_c is greater than 10, indicating at least an order-of-magnitude dominance of friction over inertia. In reservoirs, wavelengths can be short due to hydropower operations. and flow occurs at greater depths and smaller velocities than in free-flowing rivers. This combination of conditions yields a small Courant number, large channel conveyance, and small dimensionless wavelength, and F_c for reservoir waves can be significantly less than 1. When an ice cover is present, the dimensionless wavelength of a given wave and the relative magnitudes of the friction parameters increase.

The magnitude of scaling parameter D_I indicates the importance of pressure gradient effects on the wave. D_I represents the square of the ratio of the Courant number to the Froude number, and can be physically interpreted as the square of the ratio of the surface wave to the measured wave celerity. Figure 2 presents D_I as a function of Courant number for a range of Froude numbers. A value of D_I = 1 indicates that the measured wave celerity is equal to the surface wave celerity at the mean flow depth. When D_I is significantly greater than 1, measured wave celerity is much smaller than the corresponding dynamic wave celerity, generally favoring bulk wave behavior.

When the friction parameters are much greater than 1, river flow waves exhibit bulk wave behavior and, to a good approximation, eq 12 becomes

$$\frac{v^*}{y^*}\frac{\partial v^*}{\partial t^*} + \left(\frac{5}{2}\frac{v^{*2}}{y^*} - S\right) C_r \frac{\partial v^*}{\partial x^*}$$

$$= C_r Dy^* \frac{\partial^2 v^*}{\partial x^{*2}}, \qquad (13)$$

where

$$D = \frac{D_I}{F_c} = \frac{C_*^2}{2 F_0^2 (\frac{k\Delta x}{y_0})},$$

a nondimensional form of eq 7. The diffusion and kinematic wave equations are contained within the Saint-Venant system equation. For high-friction flow conditions, the bulk wave portion of the system equation is dominant, and the apparent wave celerity is that of a bulk wave. The bulk flow waves described by eq 13 are independent of the characteristic equations 3 and 4.

The bulk wave Courant number is generally greater than 0.5, as the flow velocity is only slightly less than the wave celerity. The magnitude of D relative to 1 indicates the importance of wave diffusion relative to advection. D for bulk river waves is generally less than 1, indicating that the waves are advection-dominated. With friction dominating inertia and advection dominating diffusion, the equations describing bulk waves have evolved from a second-order hyperbolic system to a dominantly hyperbolic first-order system. When $S_0 \approx S_{f_0}$, the dimensionless diffusion coefficient D varies inversely with the product of bed slope and nondimensional wavelength. D is presented in Figure 3 as a function of dimensionless wavelength for a range of Froude numbers and a dimensionless channel conveyance of about 9.

Dynamic wave behavior is indicated when the magnitude of one or both of the friction parameters is on the order of 1. As friction and inertia both make important contributions to the momentum balance, dynamic wave behavior is an intermediate condition between bulk wave and frictionless gravity wave behavior. Dynamic wave behavior occurs over a wide range of conditions, and wave subtypes can be identified that correspond to varying magnitudes of the Courant number and friction parameters.

At the transition from bulk to dynamic waves, friction is quite great. The magnitudes of F_c and C_r are both on the order of 1, and all terms of eq 12 are significant, defining the "complete equation" case. F_c on the order of 1 and $C_r << 1$ defines the "transition" case, where the flow velocity is small relative to observed wave speed and the contribution of friction is smaller than in the complete equation case. The small Courant number indicates that transition waves do not retain significant bulk wave character. The mathematical description is also simpler, as many of the terms of eq 12, including the nonlinear first-order terms, are negligible. As friction is reduced further, F_c and C_r are $<< 1$, and F_I is reduced to the order of 1. Negligible F_c indicates the lack of influence of the channel bed slope on the flow. These conditions are representative of flow in reservoirs.

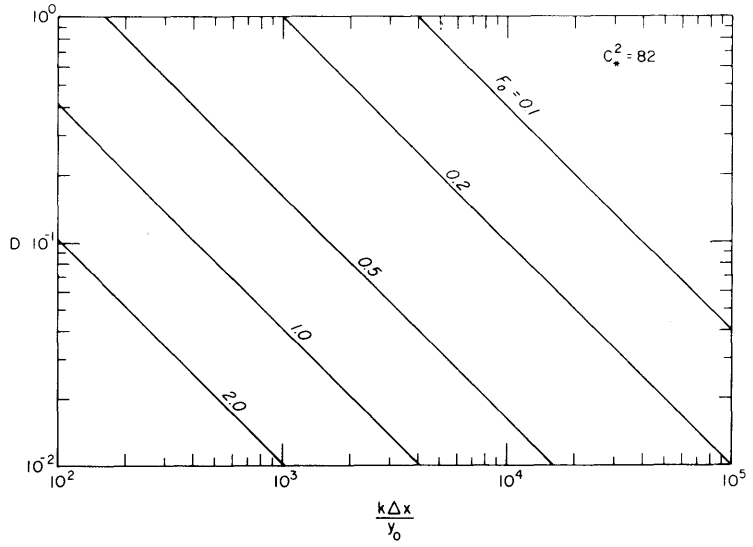

Figure 3. Dimensionless diffusion coefficient of bulk waves as a function of dimensionless wavelength for a range of Froude numbers and a typical dimensionless channel conveyance.

The dimensional system equation for the "reservoir" case is

$$\frac{\partial^2 v}{\partial t^2} - c^2 \frac{\partial^2 v}{\partial x^2} = -2\gamma \frac{\partial v}{\partial t} , \qquad (14)$$

where

$$\gamma = \frac{v}{C_*^2 R} ,$$

the familiar telegraph equation or equation of a damped vibration. Assuming that c and γ are constants, eq 14 has solutions of the form

$$v = e^{-\gamma t}\, e^{ik[x \pm c\sqrt{1 - \gamma^2/(k^2 c^2)}\; t]} \qquad (15)$$

where k is an arbitrary nonzero constant. The resistance term $\partial v/\partial t$ of eq 14 follows from the F_I term of eq 12; it provides exponential wave attenuation and retards wave celerity, separating the behavior of reservoir dynamic waves from that of gravity waves. The amplitude decay of reservoir waves is directly proportional to the magnitude of F_I, indicating a gradual transition between wave types.

Gravity wave behavior with dominant inertia occurs when friction is negligible: F_I and $F_c \ll 1$. Gravity waves, like bulk and dynamic waves, have subtypes, each of which is undamped due to the absence of friction. The "wave equation" case occurs when $C_r \ll 1$. The system equation for this case is the classical wave equation, obtained from eq 14 by setting $\gamma = 0$. Physically, this condition is approximated by a smooth, deep forebay of a hydropower station in which the flow velocity is small relative to the surface wave speed. The "simple wave" case occurs when the Courant number is on the order of 1. The method of characteristics provides a convenient formulation (eq 5, 6) for constructing solutions for this case. Positive disturbances upstream generate waves with converging characteristics, leading to wave steepening and shock formation. Wave propagation over small distances in a smooth channel may be adequately represented as a simple wave, but, as shown in Figure 1, friction increases with the Courant number eq 12, limiting the applicability of these equations.

The scaling parameter magnitudes determine wave behavior and type. The structure for understanding river wave behavior developed from our analysis is depicted in Figure 4, where the progression of wave subtypes is presented in a natural order. Only one dimensionless parameter changes in magnitude between two adjacent wave subtypes, tending from friction-dominated kinematic waves to frictionless gravity waves. The continuous dependence of the scaling parameters on the scaling variables indicates gradual transitions between wave types and subtypes.

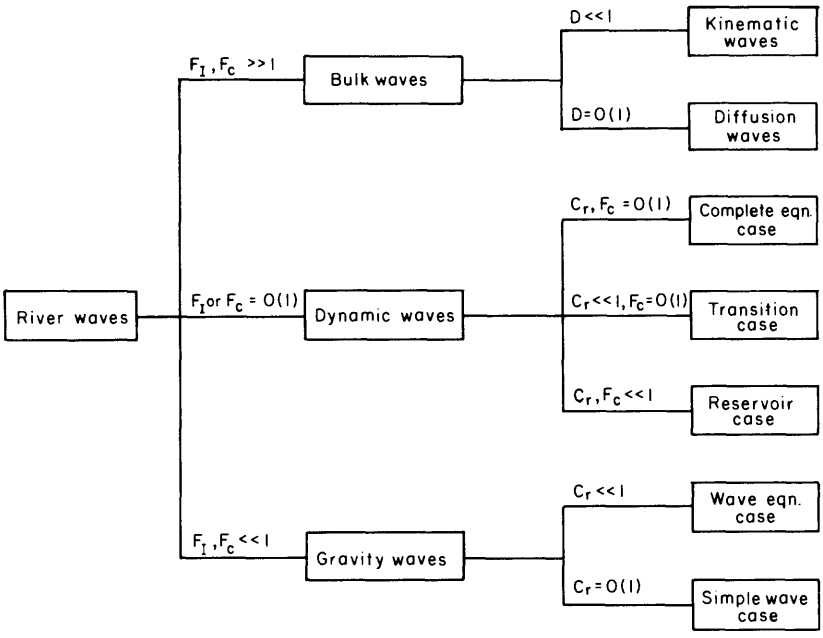

Figure 4. River wave structure obtained from the analysis of the Saint-Venant equations.

Probabilistic scaling parameters

Our analysis of the equations governing river waves provides a structure with which to consider wave behavior. Choosing representative scaling variables $v_0, y_0, \Delta x, \Delta t, C_*$, and S_0, we obtain quantitative estimates of the dimensionless scaling parameters F_I, F_c, C_r, and D_I. For cases sufficiently removed from the transitions between wave types, these intuitive, deterministic parameters may provide sufficient information to understand wave dynamics. However, assuming representative or mean scaling variables provides no information about the effects on the wave of the physical variability of the river. It could be argued that single-valued variables cannot meaningfully represent natural rivers, which have significant geometric variability. An example of this problem is attempting to characterize reservoir depth by a mean of 6 m, when depth varies between 2 m upstream and 15 m downstream. Further insight concerning the transitions between river wave types requires a more complete description of the scaling parameters than is provided by estimates of their mean values. A practical modeling requirement that has not been addressed is how to assess the confidence of wave type interpretation when scaling parameters fall near a transition.

We will now consider the more general case where scaling variables are continuous, possessing a mean and a distribution. By treating these physical quantities as random variables, probabilistic concepts can be applied. As functions of random variables, the scaling parameters are themselves random variables. Rosenblueth (1975) developed a method for estimating the first and second moments and minimum values of a function of random variables, given the first two or three moments of each variable and correlation coefficients for each pair of random variables. The estimate obtained of the mean value of the function is equivalent to a second-order Taylor series approximation, and the estimate of the coefficient of variation is a first-order approximation. The method is algebraic, replacing the distribution of each random variable by point estimates and not requiring the computation of derivatives.

Before proceeding, the Rosenblueth method for a function of two correlated random variables will be described in detail. The coefficient of variation of a random variable x is defined as

$$V_x = \frac{S_x}{\bar{x}}, \tag{16}$$

where S_x is the standard deviation of x and $\bar{x}$ is the mean. The correlation coefficient of random variables x_1 and x_2 is defined as

$$\rho = \frac{\mathrm{cov}(x_1, x_2)}{S_{x_1} S_{x_2}}, \tag{17}$$

where $\mathrm{cov}(x_1, x_2)$ is the covariance. A correlation coefficient of magnitude 1 indicates a perfect linear correlation between the variables, while a coefficient of 0 indicates uncorrelated variables. The scaling variable ranges corresponding to the propagation of a river wave through a reach are relatively small. Numerical experiments have shown that if the relationship between random variables over a limited range can be written as

$$x_1 = a\, x_2^b, \tag{18}$$

then the magnitude of ρ will be approximately 1.

In general, sufficient data will not be available to describe the precise nature of the distribution of each scaling variable. Therefore, for simplicity we will assume that these distributions are symmetric about the mean value. The point estimates representing the distribution of a scaling variable are then

$$P_{++} = P_{--} = \frac{1+\rho}{4}, \qquad P_{+-} = P_{-+} = \frac{1-\rho}{4}. \tag{19}$$

These point estimates sum to 1 and, in the case of uncorrelated random variables, are each ¼. The point estimates provide weighting factors for evaluating the function at points a standard deviation from the mean of each random variable:

$$\begin{aligned} y_{++} &= y(x_1 + S_{x_1}, x_2 + S_{x_2}), \\ y_{+-} &= y(x_1 + S_{x_1}, x_2 - S_{x_2}), \\ y_{-+} &= y(x_1 - S_{x_1}, x_2 + S_{x_2}), \\ y_{--} &= y(x_1 - S_{x_1}, x_2 - S_{x_2}). \end{aligned} \tag{20}$$

Then, the expected values or moments of the function can be obtained:

$$E[y^n] = P_{++} y_{++}^n + P_{+-} y_{+-}^n + P_{-+} y_{-+}^n + P_{--} y_{--}^n. \tag{21}$$

The expected value or mean of y is found by setting $n = 1$. The variance of y is readily computed as

$$V[y] = E[y^2] - (E[y])^2 = S_y^2. \tag{22}$$

Table 1. Application of Rosenblueth (1975) method to Liard River data.

Input: $\bar{v}_0 = 0.72$ m/s, $V_{v_0} = 0.25$, $\bar{c} = 1.4$ m/s, $V_c = 0.20$

Output: $y = C_r = 0.5357(++), 0.8036(+-), 0.3214(-+), 0.4821(--)$

	$\rho = 0.6$	$\rho = 0.8$	$\rho = 1.0$
$E[C_r]$	0.520	0.514	0.509
$V[C_r]$	0.0127	0.0067	0.0007
V_{C_r}	0.216	0.159	0.053

Rosenblueth (1975) discussed the generalization of this technique to functions of any number of random variables.

A sample calculation using Rosenblueth's procedure to obtain parameters describing the Courant number distribution for data from the Liard River (Parkinson 1981, 1982) is given in Table 1. The coefficients of variation chosen for wave celerity bound most of the observed values within one standard deviation of the mean. Because the mean flow velocity is a computed value, a relatively large coefficient of variation for velocity was assumed. Flow velocity and wave celerity for bulk flow waves can be related by an equation of the form of eq 18 and $\rho \approx 1$. However, to examine the sensitivity of the computation to the correlation coefficient, results are given in Table 1 for three different ρ values. With increasing ρ the mean Courant number decreases only slightly, but the variance and coefficient of variation decrease significantly. Estimates of the maximum and minimum values of the Courant number distribution should be greater than $C_{r_{+-}}$ and less than $C_{r_{-+}}$, respectively.

Given a function of random variables, Rosenblueth's method provides an improved estimate of the mean and estimates of scatter about the mean and the limits of the distribution. The mean, standard deviation, and limits of a random variable uniquely specify a β distribution. Harr (1977) gives the general expression for this distribution as

$$f(y) = \frac{1}{(b-a)B(\alpha+1, \beta+1)}\left(\frac{y-a}{b-a}\right)^{\alpha}\left(\frac{b-y}{b-a}\right)^{\beta} \quad (23)$$

where

$$\alpha = \frac{(\bar{y}-a)^2}{S_y^2}(1-\tilde{y}) - (1+\tilde{y}) ,$$

$$\beta = \frac{\alpha+1}{\tilde{y}} - (\alpha+2) ,$$

and

$$\tilde{y} = \left(\frac{\bar{y}-a}{b-a}\right)$$

where a and b are the minimum and maximum values of y, respectively, and B is a beta function. When α and β have the same sign, the β distribution is unimodal and bell-shaped. The coefficients of skewness and kurtosis of the β distribution can be readily obtained. With this distribution the probability of y in a given range can be determined.

To incorporate the effects of the physical variability of the river on the wave, we will use the Rosenblueth method and obtain a corresponding β distribution of the friction scaling parameters. This procedure allows further investigation of the bulk/dynamic and dynamic/gravity wave transitions and provides a reliability estimate for wave type determination when the friction parameter mean is near a transition.

Case studies

The river wave structure that has been developed depends on parameter magnitudes that are large or small relative to 1 or are on the order of 1. We will now use experience from case studies to define more precisely the parameter ranges corresponding to each wave type and transition. We will also classify a number of diverse river wave cases and consider changing wave behavior over distance to test the usefulness and practicality of our analysis.

Individual case studies and physical variables representative of each river and wave are presented in Table 2, as well as the first-order Taylor series approximations of the mean values of the scaling parameters—that is, the parameter evaluated at the mean values of all scaling variables. Estimated Manning's roughness and river bed slope values are designated in the table with an *e*. For free-flowing rivers where measured velocities were unavailable, the Chezy

equation with the characteristic depth, river bed slope, and conveyance was used to obtain a computed mean characteristic velocity, which is designated with a *c*. The mean velocity for reservoirs was computed using the continuity equation from the mean discharge, channel width, and characteristic depth.

Bulk flow waves occur when the friction parameters are sufficiently large relative to 1. Because the Courant number is by definition less than 1, F_c is always smaller than F_I and is the natural parameter to define the boundary between bulk and dynamic waves. Parkinson (1981, 1982) studies the river waves that initiated ice-cover breakup on the Liard and Mackenzie Rivers. These waves had long periods, characteristic of spring flood waves in large river systems. The bulk wave behavior that occurred is reflected in the large friction parameter magnitudes for these cases. Large values of F_c also correspond to data from open-water and flow-over-the-ice conditions in a free-flowing reach of the Ottauquechee River (Ferrick and Lemieux 1983), again indicating bulk wave behavior. Ferrick (1980) numerically modeled rapidly varied flow waves from laboratory studies of dam breaches at the Waterways Experiment Station. A wave release to a previously dry channel, corresponding to a mean F_c value of 11, was precisely simulated using a bulk wave numerical model. In addition, Ferrick et al. (1984) found that rapidly varied flow waves in the Hiwassee and Clinch Rivers, with a minimum mean F_c value of 12, behaved as bulk waves.

According to these observations, F_c greater than about 10 indicates bulk wave behavior. The system equation terms that are more than an order of magnitude smaller than the other terms are apparently negligible. With this guideline we can approximate the transitions between wave types and subtypes as corresponding to scaling parameter magnitudes greater than 10 ($>> 1$) and less than 0.1 ($<< 1$). Because the scaling parameters representing a given river reach and wave are continuous, however, any single-valued definition of a transition is inadequate. The governing equations used for analysis change between bulk, dynamic, and gravity wave conditions, and these transitions will be considered in detail.

All of the bulk wave cases have mean Courant numbers greater than 0.5 (Table 2), a necessary but apparently not sufficient condition for the occurrence of bulk waves. Table 2 also confirms that large dimensionless wavelengths favor but do not guarantee bulk wave behavior. The wave diffusion present in all cases was sufficient to prevent the formation of a shock wave or depth discontinuity at the wave front. However, as the magnitude of D approaches 0, the probability of wave steepening and shock formation increases. Only in the Clinch River was wave diffusion sufficient to produce significant wave peak attenuation. These observations support the order-of-magnitude approximation for locating the transition between the bulk wave subtypes. Mean dimensionless diffusion coefficients less than about 0.1 indicate kinematic waves, and diffusion waves occur when D is larger.

The case studies from Table 2 that bracket the bulk/dynamic wave transition $F_c = 10$ are waves having a 1-hr period on the Clinch River and a short-period wave on the Ottauquechee River that occurred immediately following ice cover breakup (moving ice). In this discussion we refer to these cases as simply Clinch River and Ottauquechee River. The extensive documentation available from the Clinch River study allows well-supported estimates of the coefficient of variation for the scaling variables. These values were chosen so that the majority of the data fall within one standard deviation of the mean, and essentially all data are within three standard deviations of the mean. With less data available from the Ottauquechee River, we assume for purposes of comparison that the coefficients of variation equal those from the Clinch River. The coefficients of variation of velocity, wave celerity, wavelength, and hydraulic depth were taken as 0.15, and as 0.20 for channel conveyance. For both cases, correlation coefficients for velocity/depth, conveyance/depth, velocity/celerity, and wavelength/celerity were specified. Observed bulk wave celerity on the Clinch River indicates a velocity/wavelength correlation. The relatively high wave celerity on the Ottauquechee River indicates dynamic wave effects, and wave celerity/depth and wavelength/depth correlations. The correlated variables for river flow are related analytically in the form of eq 18, and therefore correlation coefficients of 1 were assumed.

With these input data, Rosenblueth's method yields the mean, coefficient of variation, and minimum and maximum F_c values presented in Table 3. Table 3 also includes parameters of the β-distribution fit to F_c and probabilities of F_c in selected ranges for each case. We note that the second-order estimates of the mean for each case are significantly larger than the first-order estimates in Table 2. The relatively large coefficients of variation of F_c indicate that these distributions have significant spread. The β distributions representing the F_c distributions for the Clinch and Ottauquechee Rivers (Fig. 5) extend a significant distance on either side of the approximate transition, $F_c = 10$. Therefore, a finite probability exists that bulk or dynamic wave behavior will occur in each case. This fact implies that point estimates of F_c falling near a transition are of limited

Table 2. Case studies of river waves.

Case	$S_{o_{ave}}$ † ($\times 10^{3}$)	n_{ave} †	C^2_*	y_o/k (m)	v_o †† (m/s)	c_m (m/s)	Δx (km)	Δt	$\frac{k\Delta x}{y_o}$ ($\times 10^{-2}$)	F_o	C_r	F_l	D_l	F_c	D
WES Flume	5.0	0.009					0.125								
dry			330	0.02	0.58	1.1		110s	63	1.3	0.53	20	0.17	11	0.016
wet			530	0.08	1.4	2.3		54s	16	1.6	0.61	3.5	0.15	2.1	--
CRREL Flume															
open	0.10	0.0044	2400	0.09	0.37	0.9	0.110	120s	12	0.39	0.41	0.41	1.1	0.17	--
	0.37	0.0079	740	0.09	0.34				12	0.36	0.38	1.2	1.1	0.46	--
	1.56	0.010	460	0.08	0.52				14	0.59	0.58	3.4	0.97	2.0	--
ice	0.10	0.015	200	0.09	0.38	1.1	0.130	120s	14	0.38	0.35	5.0	0.85	1.8	--
	0.37	0.014	220	0.08	0.40				16	0.40	0.36	5.2	0.81	1.9	--
	1.56	0.014	210	0.07	0.47				19	0.47	0.43	7.5	0.84	3.2	--
Hiwassee River	5.1	0.066	23	1.0	1.1c	1.4				0.35	0.79		5.1		
1 hr							2.5	30m	25			170		130	0.038
3 hr							7.6	90m	76			510		400	0.013
Clinch River	0.36	0.026	150	1.0	0.73c	1.0				0.23	0.73		10		
1 hr							1.8	30m	18			17		12	0.81
2 hr							3.6	60m	36			34		25	0.40
Liard River ice covered	0.33	0.04	79	2.0	0.72c	1.4	180	36h	900	0.11	0.51	1100	21	560	0.037
Mackenzie River ice covered	0.12	0.03	160	3.0	0.76c	1.4	360	72h	1200	0.10	0.54	790	29	430	0.068
Ohio River	0.095	0.03													
			220	7.6	1.3c	7.5c	54	120m	71	0.15	0.17	11	1.3	1.9	--
			230	9.0	1.4c	5.6c	200	600m	220	0.15	0.25	47	2.8	12	0.24

Ottauquechee River	3.1														
open		0.04	35	0.18	0.44c	0.55	2.0	60m	110	0.33	0.80	500	5.9	400	0.015
flow over ice		0.04	49	0.47	0.84c	0.88	16	300m	340	0.39	0.95	1300	5.9	1200	0.005
fragmented cover 1		0.03e	110	0.90	0.55c	4.0	1.6	400s	18	0.13	0.14	4.4	1.2	0.62	--
fragmented cover 2		0.03e	120	1.2	0.54c	3.2	1.3	400s	11	0.11	0.17	3.0	2.4	0.51	--
moving ice		0.05e	50	1.9	1.3c	2.8	1.7	600s	9	0.30	0.46	16	2.3	7.4	--
St. Lawrence River	0.04e	0.03	180	4.5	0.6	8.2				0.064	0.073		1.3		
ice covered															
2 hr							30	60m	67			5.3		0.39	--
6 hr							89	180m	200			16		1.2	--
Old Hickory Reservoir	--	0.032	190	6.5	0.14	7.3				0.018	0.019		1.2		
2 hr							26	60m	40			0.80		0.015	--
4 hr							52	120m	80			1.6		0.030	--
Pine Falls Reservoir	--	0.025e													
ice covered															
upstream portion			210	2.1	0.40	2.0	7.2	60m	34	0.063	0.20	6.5	9.9	1.3	--
downstream portion			280	4.9	0.17	3.9	14	60m	29	0.017	0.044	0.91	6.3	0.040	--
Wheeler Reservoir	--	0.028	240	5.9	0.20	6.7				0.026	0.030		1.3		
2 hr							24	60m	41			1.0		0.030	--
4 hr							48	120m	81			2.0		0.060	--

†e = estimated Manning's roughness and river bed slope values.

††c = Chezy equation used, with characteristic depth, river bed slope, and conveyance.

Table 3. Bulk/dynamic wave transition.

Case	$\bar{F}_c$	V_{F_c}	$F_{c_{min}}$	$F_{c_{max}}$	α	β	$P[F_c<8]$	$P[F_c<10]$	$P[F_c<12]$
Clinch River	15.1	0.477	3.0	50	0.838	4.30	0.17	0.28	0.39
Ottauquechee River	8.75	0.375	2.0	30	1.97	8.35	0.46	0.68	0.84

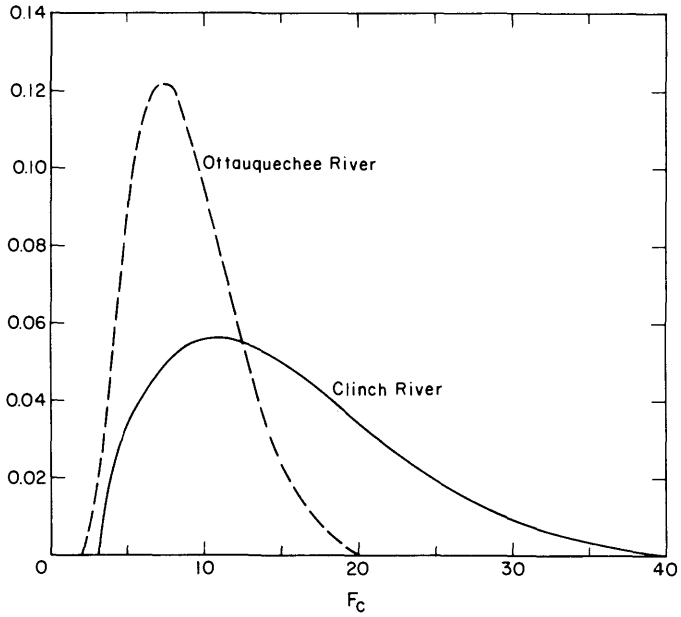

Figure 5. Probability distributions of friction scaling parameter F_c representing case studies of the Clinch River and the Ottauquechee River.

value as indicators of wave type, and emphasizes that the transitions between wave types in rivers are continuous. If we consider the transition range $8 \leq F_c \leq 12$, the ratio of probabilities, R_1, of bulk-to-dynamic wave behavior for F_c outside this range is

$$R_1 = \frac{P[F_c > 12]}{P[F_c < 8]} \quad . \tag{24}$$

Values of R_1 near 1 do not identify wave type, but progressively larger deviations from 1 indicate wave type with increasing reliability. In our case, R_1 (Clinch) = 3.6 and R_1 (Ottauquechee) = 0.35, indicating probable bulk wave behavior and probable dynamic wave effects, respectively. The diagnosis of Clinch River bulk wave behavior is strongly supported by modeling results (Ferrick et al. 1984).

Dynamic waves span a range of the friction parameters of about two orders of magnitude. The scaling parameter bounds that identify complete-equation dynamic waves are roughly defined as $F_c < 10$ and $C_r > 0.1$. In these relatively high friction cases, where dynamic waves typically result from some rapidly varying initial condition, frictional effects can eventually restore bulk wave behavior. Downstream-propagating waves following a dam breach or the sudden release of an ice jam are examples of such cases. Stoker (1957) simulated the propagation of the front of a hypothetical, rapidly varying, large-amplitude flood wave on the Ohio River using the dynamic wave equations. At the upstream boundary he imposed a 1.5-m/hr rise in the water level for a 4-hr period between initial and final steady-flow conditions. The magnitudes of the friction parameters and the Courant number for 2 hr after the initiation of the wave (Table 2) indicate significant inertia. However, average scaling variables representative of the first 10 hr of the simulation yield mean friction parameters in the bulk wave range. Mean scaling variables representing the latter part of this time period produce even larger friction parameter magnitudes and a mean Courant number greater than 0.5.

Stoker stated that prior to his work more gradual flood waves recorded on the Ohio River had been successfully described with bulk wave models, as would be expected based on our analysis.

The other complete-equation dynamic wave cases given in Table 2 are predominantly rapidly varying flow waves with small dimensionless wavelengths. This group of cases includes a laboratory dam breach release to a channel with a significant base flow (WES flume-wet), laboratory studies (Ferrick 1984) of the effects of bed slope and ice cover upon a sequence of flow waves (CRREL flume), and three waves on the Ottauquechee River immediately prior to and during ice cover breakup. The laboratory flume cases each had bulk measured wave speeds, but because of very smooth channels the friction parameters fall in the dynamic wave range. At break-up the Ottauquechee study reach was ponded to a large depth relative to wave amplitude. The channel conveyance at the breakup was much smaller than in the laboratory studies, but the measured river wave celerities approached those of dynamic waves and are reflected in small Courant numbers. The upstream half of ice-covered Pine Falls reservoir (Kartha 1976) is a complete-equation dynamic wave case that did not involve a short-period flow wave. However, a large channel conveyance and a low flow velocity relative to measured wave celerity compensate for a relatively large dimensionless wavelength.

The Courant number for the transition dynamic wave case is smaller than that for the complete equation case, and the friction parameter F_c is also generally smaller. The dimensionless scaling parameter bounds that identify transition dynamic waves are roughly defined as $F_c > 0.1$ and $C_r < 0.1$. Waves of 2-hr and 6-hr durations in the ice-covered St. Lawrence River between Lake Ontario and Cardinal, Ontario (Yapa 1983), are examples of transition-case dynamic waves. The observed wave celerity was that of a dynamic wave and was much greater than the flow velocity.

The reservoir dynamic wave case is characterized by a small flow velocity relative to measured wave speed and relatively small frictional effects. This case is roughly defined by dimensionless parameters F_c and $C_r < 0.1$. In Table 2 waves from hydroelectric power generation in Old Hickory Reservoir on the Cumberland River (Ferrick 1979), in the downstream half of Pine Falls Reservoir on the Winnipeg River (Kartha 1976), and in Wheeler Reservoir on the Tennessee River (Ferrick and Waldrop 1977) are reservoir waves. Wave propagation in the upstream portion of the Old Hickory and Wheeler Reservoirs is subject to larger frictional effects than farther downstream and, if analyzed separately, would be classified as a higher-friction dynamic wave type. For each of these cases friction remains important, as velocity decay to 10% of the original amplitude occurs within a 4- to 6-hr period (eq 15).

The case studies compiled in Table 2 do not include a case that falls in the gravity wave range. The reservoir dynamic waves are the smallest friction cases available, with estimated mean F_I values of about 1 from the Old Hickory, Pine Falls, and Wheeler Reservoir data. We will use the 2-hr wave period data from Wheeler Reservoir to consider the dynamic/gravity wave transition. A treatment of this boundary consistent with that used for the bulk/dynamic wave transition provides values of F_I between 0.083 and 0.125 as the transition range. Table 4 presents wave amplitude decay times of 2-hr period waves on Wheeler Reservoir for F_I as computed and bounding the transition. The actual conditions are far removed from the transition.

The scaling variables presented in Table 2 for Wheeler Reservoir are mean values for the complete reservoir. These values, repeated in Table 5 along with estimated coefficients of variation, provide input for the Rosenblueth method. Wheeler is a typical reservoir in that dramatic changes in depth and flow velocity occur over its length, reflected in large coefficients of variation. If we partition the reservoir and consider the 40-km reach farthest downstream, this physical variability is greatly reduced. All coefficients of variation are reduced by roughly a factor of 2, which, for purposes of comparison,

Table 4. Wave amplitude decay time (hr).

Amplitude/A_0	*F_I = 1.0*	*F_I = 0.125*	*F_I = 0.083*
0.9	0.2	1.7	2.5
0.5	1.4	11	17
0.1	4.6	37	55

Table 5. Input data for Rosenblueth's method.

	Wheeler Reservoir (complete)		*Wheeler Reservoir (downstream)*	
Variable	$\bar{x}$	V_x	$\bar{x}$	V_x
y_0(m)	5.9	0.25	8.0	0.125
v_0(m/s)	0.2	1.0	0.1	0.5
C_*	15.5	0.02	15.5	0.01
c_m(m/s)	6.7	0.15	8.5	0.075
Δx(m)	24,000	0.15	31,000	0.075

Table 6. Dynamic/gravity wave transition.

Case	$\bar{F}_I$	V_{F_I}	$F_{I_{min}}$	$F_{I_{max}}$	α	β	$P[F_I<0.083]$	$P[F_I<0.100]$	$P[F_I<0.125]$
Wheeler Reservoir	0.65	0.457	0.0	3.8	2.8	17.5	0.0017	0.0033	0.0070
Wheeler Reservoir (downstream)	0.35	0.268	0.0	1.0	7.7	15.4	0.0001	0.0005	0.0025

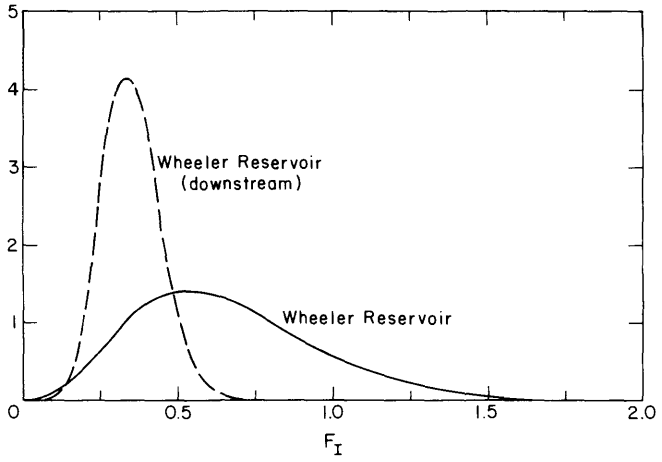

Figure 6. Probability distributions of friction scaling parameter F_I representing case studies of Wheeler Reservoir and the downstream portion of Wheeler Reservoir.

we assume is exactly the case. In addition, the mean flow depth in the lower portion of the reservoir is greater and the velocity is smaller than values representing the complete reservoir, moving F_I toward the dynamic/gravity wave transition. These data are also given in Table 5. The correlation coefficients used in the method were identical to those for dynamic waves in the Ottauquechee River.

Presented in Table 6 are parameters of the F_I distribution for both cases from the Rosenblueth method, parameters describing a β-distribution fit to F_I, and probabilities bounding and within the dynamic/gravity wave transition. The second-order estimate of the mean for the complete reservoir is a third smaller than the first-order estimate given in Table 2. The mean F_I of the downstream portion is about one-half the value for the complete reservoir, with a significantly smaller coefficient of variation. The ratio

$$R_2 = \frac{P[F_I > 0.125]}{P[F_I < 0.083]}, \qquad (25)$$

where a large value of R_2 relative to 1 indicates dynamic wave behavior and an R_2 value much less than 1 indicates gravity wave behavior, reveals that neither case approaches the wave transition. The pronounced difference in spread between the F_I distributions and the small probability that F_I is less than 0.1 can be readily seen with a plot of these distributions (Fig. 6). These results demonstrate that river waves in reservoirs may resemble gravity waves over small distances, but waves propagating more than a few wavelengths are significantly affected by friction.

CONCLUSIONS

The Saint-Venant system equation, formed by combining the continuity and momentum equations, contains a pair of wave celerities. The dynamic wave celerity is associated with the second-order terms, which are due to inertia and the pressure gradient, and the kinematic wave celerity is associ-

ated with the first-order terms, which are due to bed slope and friction. River wave behavior is controlled by the balance between friction and inertia. The nondimensional scaling parameters of the Saint-Venant system equation can be used to quantify this balance. The dimensionless parameters define a spectrum of river waves, with continuous transitions between wave types and subtypes. Dynamic, gravity, diffusion, and kinematic waves correspond to specific scaling parameter ranges of this spectrum. Bulk waves occur when the friction terms of the system equation dominate the inertia terms. Dynamic waves occur when the second-order inertia terms of the system equation are significant. Because friction in rivers is generally important, there are few cases where the inertia terms dominate the friction terms and river waves behave as gravity waves.

The parameter range corresponding to each wave type and transition was defined using data from case studies, allowing direct application of the scaling parameters for identification of wave type. The capability to identify wave type is necessary to the construction of appropriate mathematical models of river flow. Changes in wave behavior with propagation distance for rapidly varying initial flow conditions and changes resulting from the presence of an ice cover can be addressed quantitatively using the scaling parameters. Interpreting the scaling parameters as random variables supplies the generality needed to consider waves in rivers with significant physical property ranges and provides a measure of the reliability of wave type assessments near a transition.

LITERATURE CITED

Courant, R. and K.O. Friedrichs (1948) *Supersonic Flow and Shock Waves.* New York: Interscience, p. 1-70.

Cunge, J.A., F.M. Holly, Jr. and A. Verwey (1980) *Practical Aspects of Computational River Hydraulics.* Marshfield, Massachusetts: Pitman, p. 357-360.

Ferrick, M.G. (1979) A flow routing model for Old Hickory Reservoir. TVA Water Systems Development Branch Report No. WR28-1-89-102.

Ferrick, M.G. (1980) Flow routing in tailwater streams. In *Computer and Physical Modeling in Hydraulic Engineering* (G. Ashton, Ed.). New York: American Society of Civil Engineers, p. 192-208.

Ferrick, M.G. (1984) Analysis of rapidly varying flow in ice-covered rivers. *Proceedings, IAHR Ice Symposium,* Hamburg, Germany, Vol. 1, p. 359-368.

Ferrick, M.G. and W.R. Waldrop (1977) Two techniques for flow routing with application to Wheeler Reservoir. TVA Water Systems Development Branch Report No. 3-519.

Ferrick, M.G. and G.E. Lemieux (1983) Unsteady river flow beneath an ice cover. In *Frontiers in Hydraulic Engineering* (H.T. Shen, Ed.). New York: American Society of Civil Engineers, p. 254-260.

Ferrick, M.G., J. Bilmes and S.E. Long (1984) Modeling rapidly varied flow in tailwaters. *Water Resources Research,* **20**: 271-289.

Harr, M.E. (1977) *Mechanics of Particulate Media, A Probabilistic Approach.* New York: McGraw-Hill, 543 pp.

Henderson, F.M. (1963) Flood waves in prismatic channels. *Journal of the Hydraulics Division of the American Society of Civil Engineers,* **89**(HY4): 39-67.

Hildebrand, F.B. (1962) *Advanced Calculus for Applications.* Englewood Cliffs, New Jersey: Prentice-Hall, Inc., p. 400-410.

Kartha, C.V. (1976) Flow fluctuation tests, Winnipeg River redevelopment hydrology report no. 2. Manitoba Hydro, Hydro Development Department, Report No. 76-20.

Menendez, A.N. and R. Norscini (1982) Spectrum of shallow water waves: An analysis. *Journal of Hydraulics Division of the American Society of Civil Engineers,* **108**(HY1): 75-94.

Parkinson, F.E. (1981) Liard-Mackenzie winter regime study, observations of 1981 break-up. LHL Report 823, B.C. Hydro and Power Authority, Vancouver, B.C.

Parkinson, F.E. (1982) Liard-Mackenzie winter regime study, observations of 1982 break-up. LHL Report 886, B.C. Hydro and Power Authority, Vancouver, B.C.

Ponce, V.M. and D.B. Simons (1977) Shallow wave propagation in open channel flow. *Journal of Hydraulics Division of the American Society of Civil Engineers,* **103**(HY12): 1461-1476.

Rosenblueth, E. (1975) Point estimates for probability moments. In *Proceedings of the National Academy of Science USA,* Vol. 72, p. 3812-3814.

Stoker, J.J. (1957) *Water Waves.* New York: Interscience, p. 482-509.

Woolhiser, D.A. and J.A. Liggett (1967) Unsteady one-dimensional flow over a plane—the rising hydrograph. *Water Resources Research,* **3**: 753-771.

Yapa, P.N.D.D. (1983) Unsteady flow simulation of rivers with an ice cover. Doctoral dissertation, Clarkson College of Technology, Potsdam, New York.